

# A Physics-Enhanced Data-Driven Nonlinear Model Predictive Control Strategy for Energy Regenerative Active Suspension

Aidan Aalund<sup>1</sup>, Anye Zhou<sup>2</sup>, and Zejiang Wang<sup>\*3</sup>

**Abstract**—Vehicle suspension systems play a critical role in improving ride comfort by isolating the passenger cabin from road disturbances and enhancing vehicle handling by regulating the contact force between the wheel and the road. Active suspension, which introduces a force generator between the sprung and the unsprung masses, yields superior ride comfort and road handling than the traditional passive suspension. However, the actuation of an active suspension involves significant energy consumption. To address this challenge, Energy Regenerative Active Suspensions (EARS) have emerged, offering a promising solution by converting a portion of the dissipated vibrational energy into electricity. However, controlling EARS effectively requires accurate system modeling, which can be difficult due to variable suspension parameters, such as spring aging or changes in vehicle load. To tackle this, we develop a physics-enhanced data-driven nonlinear model predictive control strategy for EARS, with two primary control objectives: (1) Regulating suspension travel to its nominal value for ride comfort and road holding, and (2) Minimizing the overall energy consumption of the active suspension system. Our key innovation lies in the use of a physics-enhanced ultra-local model to represent the dynamics of the EARS system. Simulation results demonstrate that by replacing the physics-based model by the proposed physics-enhanced ultra-local model, the same nonlinear MPC setting yields improved suspension travel control performance, energy saving, and computational efficiency.

## I. INTRODUCTION

Suspension system is a vital component of modern vehicles, serving two primary functions: improving passenger comfort by isolating the cabin from road disturbances, and enhancing vehicle handling by ensuring optimal contact between the tires and the road. Traditionally, passive suspensions have been widely used to achieve these objectives. They rely on hydraulic-mechanical dampers and springs to absorb and dissipate vibrations caused by road irregularities. However, passive suspensions cannot adapt to varying road conditions, and they dissipate vibrational energy as heat, resulting in energy loss.

In response to these limitations, active suspension systems have been developed. Unlike passive systems, active suspension uses actuators to dynamically adjust suspension forces, allowing for superior control of ride comfort and road holding under varying driving conditions. This makes them particularly beneficial for enhancing vehicle stability and passenger comfort. However, the significant drawback

of active suspensions is their high energy consumption. This concern is especially critical in electric vehicles (EVs), where energy efficiency is paramount to maximize driving range. The energy demand of traditional active suspensions presents a major obstacle to their widespread adoption in EVs.

To address this challenge, Energy Regenerative Active Suspensions (EARS) have been proposed. EARS combine the performance benefits of active suspension with the ability to harvest and regenerate energy from suspension vibrations. By converting a portion of the dissipated vibrational energy into usable electricity, EARS can enhance the overall energy efficiency of the vehicle, making them an appealing solution for next-generation EVs. Various research efforts have explored different energy harvesting mechanisms for EARS, such as electromagnetic generators and energy harvesting shock absorbers (EHSAs). These systems demonstrate the potential to recover significant amounts of energy, with studies showing fuel efficiency improvements of up to 0.8% through energy regeneration.

However, controlling EARS presents new challenges. The effectiveness of EARS relies on accurate modeling of the suspension system's dynamics, but these models are often difficult to obtain in practice. Suspension parameters, such as spring stiffness, damping coefficients, and payload, can vary due to factors like spring aging and cargo movement. This parameter variability makes traditional model-based control approaches less effective, as they require precise knowledge of the suspension system's characteristics.

To overcome these challenges, we propose a data-driven Nonlinear Model Predictive Control (NMPC) approach for EARS. Our approach leverages a physics-enhanced ultra-local model, which provides a more flexible and adaptive representation of the suspension system dynamics. This ultra-local model does not rely on precise system identification but instead continuously adapts based on real-time data, making it robust to changes in system parameters. By formulating the control problem as a constrained nonlinear optimization, we aim to achieve two key objectives: (1) regulate the suspension travel to simultaneously prevent excessive sprung mass acceleration and maintain adequate tire-road contact, and (2) minimize the overall energy consumption of the active suspension system.

Simulation results demonstrate that by replacing a traditional physics-based model with the proposed physics-enhanced ultra-local model, the same nonlinear MPC formulation yields improved performance in terms of suspension travel control, energy efficiency, and computational efficiency.

<sup>1</sup>Chandra Family Department of Electrical and Computer Engineering, The University of Texas at Austin, Austin, Texas, USA  
aidan.aalund@utexas.edu

<sup>2</sup>Buildings and Transportation Science Division, Oak Ridge National Laboratory, Oak Ridge, Tennessee, USA zhoua@ornl.gov

<sup>3</sup>Department of Mechanical Engineering, The University of Texas at Dallas, Richardson, Texas, USA zejiang.wang@utdallas.edu

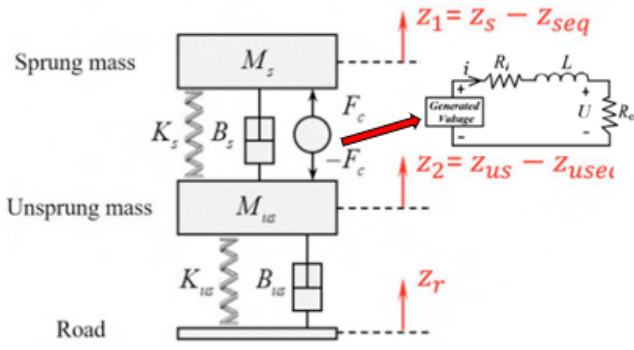


Fig. 1. Energy Regenerative Active Suspension.

## II. ENERGY REGENERATIVE ACTIVE SUSPENSION MODELING

An EARS, as displayed in Fig. 1, integrates an active suspension system, which actively controls suspension forces for optimized ride comfort and handling, with an energy harvesting system that captures suspension-generated energy and converts it into electrical power for improved energy efficiency. This is often achieved using electromagnetic or piezoelectric transducers. As the suspension compresses and rebounds, instead of dissipating the energy as heat, the harvesting system regenerates it. The recovered energy can either be stored in onboard batteries or reused to power the actuators in the active suspension, increasing overall vehicle energy efficiency.

Same to a typical active suspension system, the EARS can be described separately as the sprung mass and the unsprung mass:

$$\ddot{z}_1 = \frac{K_s}{M_s}(z_2 - z_1) + \frac{B_s}{M_s}(\dot{z}_2 - \dot{z}_1) + \frac{F_c}{M_s} \quad (1)$$

$$\ddot{z}_2 = -\frac{F_c}{M_{us}} + \frac{K_{us}}{M_{us}}(z_r - z_2) + \frac{B_{us}}{M_{us}}(\dot{z}_r - \dot{z}_2) - \frac{K_s}{M_{us}}(z_2 - z_1) - \frac{B_s}{M_{us}}(\dot{z}_2 - \dot{z}_1) \quad (2)$$

In (1) and (2),  $z_1$  and  $z_2$  are the displacements of the sprung and unsprung mass w.r.t. their equilibrium positions  $z_{seq}$  and  $z_{useq}$ .  $z_r$  is the road displacement.  $F_c$  indicates the actuation force. EARS parameters include the suspension stiffness  $K_s$ , sprung mass  $M_s$ , suspension damping  $B_s$ , tire stiffness  $K_{us}$ , unsprung mass  $M_{us}$ , and tire damping  $B_{us}$ .

In parallel, the energy regenerative actuator is mounted on the vehicle's frame. When the actuator's force aligns with the motor's rotation, the system operates in motor mode, consuming power. If the force opposes the motor's rotation, it switches to generator mode, producing energy. With an energy conversion efficiency  $\epsilon$ , we can formulate the energy consumption and generation from the actuator as:

If  $F_c(t)[\dot{z}_1(t) - \dot{z}_2(t)] \geq 0$ , the energy consumption rate of the EARS system is:

$$P_{con}(t) = \frac{F_c(t)}{\epsilon}[\dot{z}_1(t) - \dot{z}_2(t)]dt \geq 0 \quad (3)$$

Instead, if  $F_c(t)[\dot{z}_1(t) - \dot{z}_2(t)] < 0$ , the energy generation rate of the EARS system is:

$$P_{gen}(t) = \epsilon F_c(t)[\dot{z}_1(t) - \dot{z}_2(t)]dt < 0 \quad (4)$$

Therefore, from the start time  $t_0$  to the end time  $t_f$ , the overall energy consumption of the EARS reads:

$$E_{con} = \int_{t_0}^{t_f} P_{gen}(\tau) + P_{gen}(\tau)d\tau \quad (5)$$

## III. FROM ULTRA-LOCAL MODEL TO PHYSICS-ENHANCED ULTRA-LOCAL MODEL

Based on the EARS dynamics (1) and (2), as well as the energy consumption formulation (5), we formulate our control problem as:

*Determine the actuation force  $F_c$ , such that the suspension travel  $z_1 - z_2$  can remain close to zero under the influence of the road excitation  $z_r$ , while minimizing the overall energy consumption of the EARS.*

We adopt a Model Predictive Control (MPC) framework to handle this problem. The foundation of an MPC is an accurate system model, which predicts the system behavior under an optimal control sequence. Although the EARS dynamics (1) and (2) are available, its parameters can easily diverge from their nominal values. Instead of adding complex parameter identification mechanism into the overall control architecture, we adopt an ultra-local model [2] to describe the relationship between the travel displacement  $z_1 - z_2$  and the actuation force  $F_c$ . For simplicity, we define  $y = z_1 - z_2$  and  $u = F_c$ .

The ultra-local model represents the system's output  $y$ 's derivative as the sum of the weighted input  $u$  and a piecewise constant offset term [3]:

$$y^{(v)}(\tau) = F(\tau) + \alpha u(\tau). \quad (6)$$

In (6),  $y^{(v)}(\tau)$  is the  $v$ -th order derivative of the measured system output  $y(\tau)$ ,  $\alpha u(\tau)$  represents the amplified system input multiplied by a constant control gain  $\alpha$ , and  $F(\tau)$  is the offset term, which groups both the unmodeled system dynamics and external disturbances.

$F(\tau)$  is updated at each sampling step since the ultra-local model can only represent system dynamics for a small time. This can be represented as:

$$F(\tau) \approx \hat{F}(\tau) = \hat{y}^{(v)}(\tau) - \alpha u(\tau - T_s), \quad (7)$$

where  $u(\tau - T_s)$  is the last step's command with a sampling period  $T_s$ .  $\hat{y}^{(v)}(\tau)$  is the estimated  $v$ -th order derivative of the measured system output  $y(\tau)$ .

For example, with the order output derivative set as  $v = 1$ , we utilize algebraic derivative estimation from (ADE) [1] to express the derivative of  $y(\tau)$  as a time-weighted integral. ADE formulates  $\hat{y}(\tau)$  as:

$$\hat{y}(\tau) = \frac{6}{T_{ADE}^3} \int_0^{T_{ADE}} (T_{ADE} - 2t)y(\tau - t)dt. \quad (8)$$

In (8),  $T_{ADE}$  is the window size. For implementation on digital systems,  $T_{ADE}$  must be an integer multiple of  $T_s$ .

As an added benefit, the integral adds a low-pass filter effect to mitigate signal noise. Noise is common in sensors used to measure inputs in control system, making ADE suitable for control applications. This is an advantage over direct differentiation. Substituting (7) into (6) yields:

$$\begin{aligned} y^{(v)}(\tau) &\approx \hat{y}^{(v)}(\tau) - \alpha u(\tau - T_s) + \alpha u(\tau) \\ &= \hat{y}^{(v)}(\tau) + \alpha \Delta u(\tau), \end{aligned} \quad (9)$$

where  $\Delta u(\tau)$  is the control increment at time  $\tau$ .

Equation (9) can be further discretized as:

$$y_{k+1|k} = y_{k|k} + T_s \hat{y}[k] + \alpha T_s \Delta u_{k|k} \quad (10)$$

where  $y_{k|k}$  and  $y_{k+1|k}$  represents the measured system output at the current ( $k$ ) and next ( $k+1$ ) steps respectively.  $\Delta u_{k|k}$  is the control increment at step  $k$ .

In practice, the difficulties in implementing the ultra-local model (6) boils down to determining the relative degree  $v$  and the control gain  $\alpha$ . However, by subtracting (2) from (1), we get:

$$\ddot{z}_1(t) - \ddot{z}_2(t) = \ddot{y}(t) = \left(\frac{1}{M_c} + \frac{1}{M_{us}}\right)F_c(t) + F(t), \quad (11)$$

where  $F(t)$  encompasses both the modeling error caused by the suspension parameters change and the the external disturbances. Therefore, we can naturally determine  $v = 2$  and  $\alpha = \frac{1}{M_c} + \frac{1}{M_{us}}$ . We call (11) the physics-enhanced ultra-local model, which falls into the HEOL setting recently proposed by the inventors of the ultra-local model.

#### IV. EARS CONTROL BASED ON THE PHYSICS-ENHANCED ULTRA-LOCAL MODEL

In this Section, we illustrate how to formulate a nonlinear MPC based on the physics-enhanced ultra-local model (11).

Following (9), the model at each time step is:

$$\begin{aligned} \ddot{y}(t) &\approx F_{F_c}(t) + \alpha F_c(t), \\ &= \hat{\ddot{y}}(t) - \alpha F_c(t-1) + \alpha(F_c(k-1) + \Delta F_c(t)) \\ &= \hat{\ddot{y}}(t) + \alpha \Delta F_c(t) \end{aligned} \quad (12)$$

We assign  $x(t) = [y(t), \dot{y}(t)]^T$ ,  $u(t) = \Delta F_c(t)$  as the model states and input respectively. In (12),  $\hat{\ddot{y}}$  is obtained from applying the ADE (8) twice.  $\Delta F_c(t)$  is the force increment. By discretizing (12) with sample time  $T_s$ , we have:

$$\begin{bmatrix} y_{k+1|k} \\ \dot{y}_{k+1|k} \end{bmatrix} = \begin{bmatrix} 1 & T_s \\ 0 & 1 \end{bmatrix} \begin{bmatrix} y_{k|k} \\ \dot{y}_{k|k} \end{bmatrix} + \begin{bmatrix} 0 \\ \alpha T_s \end{bmatrix} \Delta F_{ck|k} + \begin{bmatrix} 0 \\ \hat{\dot{y}}_{k|k} T_s \end{bmatrix}, \quad (13)$$

which can be compacted to:

$$x_{k+1|k} = A x_{k|k} + B u_{k|k} + d(k). \quad (14)$$

With (13), the travel controller problem under the physical

constraints can be formulated in (15) and (16).

$$\begin{aligned} \arg \min_{\Delta u_{k+i|k}} J &= \sum_{i=1}^{H_p} \|y_{k+i|k} - y_{k+i|k}^r\|_Q^2 + \\ &\sum_{i=1}^{H_p} \|\dot{y}_{k+i|k} - \dot{y}_{k+i|k}^r\|_{Q_{dot}}^2 + \sum_{i=0}^{H_c-1} \|\Delta u_{k+1|k}\|_R^2 + \\ &\gamma_i T_s \sum_{i=0}^{H_p+1} \dot{y}_{k+i|k} (\Delta u_{k+i|k} + U[k-1]), \end{aligned} \quad (15)$$

where  $\gamma_i = 1/\epsilon$  if  $\dot{y}_{k+i|k}(\Delta u_{k+i|k} + U[k-1]) \geq 0$  and  $\gamma_i = -\epsilon$  if  $\dot{y}_{k+i|k}(\Delta u_{k+i|k} + U[k-1]) < 0$ .

s.t.

$$\begin{cases} x_{k+1|k} = A x_{k|k} + B u_{k|k} + d(k), & i = 0, \dots, H_p, \\ -\Delta F_{c \max} \leq \Delta u_{k+i|k} \leq \Delta F_{c \max}, & i = 0, \dots, H_c - 1, \\ \Delta u_{k+i|k} = 0, & i = H_c, \dots, H_p, \\ y_{\min} \leq y_{k+i|k} \leq y_{\max}, & i = 1, \dots, H_p + 1, \\ F_{\min} \leq U(k-1) + \sum_{i=0}^n \Delta u_{k+1|k} \leq F_{\max}, & n = 0, \\ \vdots & \vdots \\ F_{\min} \leq U(k-1) + \sum_{i=0}^n \Delta u_{k+1|k} \leq F_{\max}, & n = H_c - 1 \end{cases} \quad (16)$$

The first and second terms in the cost function (15), weighted by  $Q$  and  $Q_{dot}$  respectively, aim to minimize tracking error of the reference trajectory and its derivative within the prediction horizon. The third term, weighted by  $R$ , penalizes fluctuation of  $u$  within the control horizon. The last item corresponds to the overall energy consumption within the prediction horizon. Note that at each step within the prediction horizon, depending on the working mode of the actuator, the EARS may consume or regenerate energy.

Then, the constraints<sup>16</sup> encompass the physics-enhanced data-driven model dynamics, control increment limits, enforcement of a control horizon, control magnitude limits, and system output limits, in order. This will ensure the controller does not create a command that the actuator cannot physically produce.

Because of the energy generation term, we use `fmincon` to solve the constrained nonlinear optimization problem to obtain  $\Delta u_{k+i|k}^*$ . Finally, the optimal command is found from adding the previous command and the optimal increment at the current step.

As a benchmark, we design a traditional model-based MPC by adopting exactly the same setting in (15) and (16). The only difference lies in replacing the data driven model by the physics-based model with four states, derived from (1) and (2).

#### V. SIMULATION

##### A. Simulation configuration

For simplicity, the two nonlinear MPCs were formulated by leveraging the Matlab Model Predictive Control Toolbox. The nominal parameters of the EARS dynamics were modeled after a prototype suspension from Quanser. Additional parameters are shown in Table I.

Item	Value
Prediction Horizon	20
Control Horizon	1
Sample Time ( $T_s$ )	0.01 s
ADE window size ( $T_{ADE}$ )	$8 \cdot T_s$ s
$\alpha$	1.41
$Q$	1000
$Q_{dot}$	5
$R$	10
$E$	5
Maximum Displacement	$\pm 0.05$ m
Maximum Actuator Force	$\pm 15$ N
Maximum Change in Force	$\pm 1000 T_s$ N/s
Sprung Mass	2.45 Kg
Unsprung Mass	1 Kg
Spring Stiffness (Sprung)	900 N/m
Suspension Damping (Sprung)	7.5 Ns/m
Spring Stiffness (Unsprung)	2500 N/m
Suspension Damping (Unsprung)	5 Ns/m

TABLE I  
SIMULATION PARAMETERS

## B. SIMULATION RESULTS

The tracking performance of both the data-driven NMPC and the model-based NMPC is compared in Fig. 2

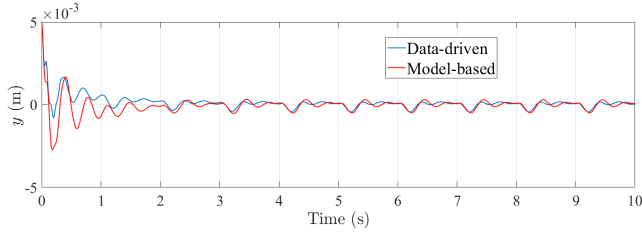


Fig. 2. Tracking performance comparison.

We can see that the data-driven controller yields improved tracking performance. This is mainly because the model-based controller can be easily impacted by the modelling errors introduced by the inaccurate model parameters. Instead, the data-driven MPC, which leverages a physics-enhanced ultra-local model, can easily handle the discrepancies between the nominal model parameters and the actual model parameters.

Then, the overall energy consumption of the EARS under investigation is depicted in Fig. 3.

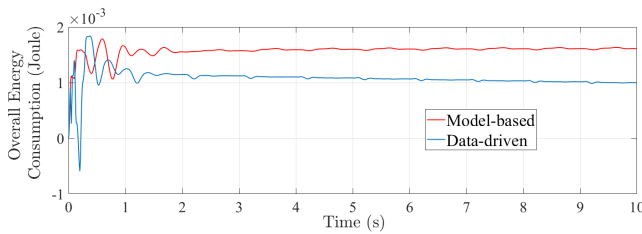


Fig. 3. Energy consumption comparison.

Again, the data-driven controller yields improved energy saving, evidenced by its reduced magnitude. By accurately predicting the model outputs, the data-driven MPC can make

MPC	Call Time	Execution Time (second)
Data-driven MPC	2013	12.3
Model-based MPC	2013	45.5

TABLE II  
EXECUTION TIME COMPARISON

informed decision to minimize the overall energy consumption.

Finally, the computational efficiency of the two MPCs are compared in Table II.

Both MPCs were triggered 2013 times, but their overall task turnaround times (TATs) were quite different. The data-driven MPC, thanks to its reduced problem size, entails an average TAT as 6ms. In contrast, the average TAT of the model-based NMPC reached 22.6ms. Clearly, adopting the data-driven MPC can further guarantee the real-time performance of the EARS.

## VI. CONCLUSIONS

In this paper, we developed a novel physics-enhanced nonlinear ultra-local model predictive control (NULMPC) strategy for Energy Regenerative Active Suspension (EARS) systems. The proposed control strategy effectively addresses the challenge of variable suspension parameters, such as spring aging or changing vehicle loads, which complicate accurate system modeling. By incorporating a physics-enhanced ultra-local model, the NULMPC regulates suspension travel to improve ride comfort and road handling, while minimizing the energy consumption of the active suspension system. Simulation results demonstrate that our approach outperforms traditional nonlinear MPC methods, yielding superior performance in terms of suspension travel control, energy efficiency, and computational cost. These findings suggest that our NULMPC strategy offers a promising solution for optimizing EARS, paving the way for more energy-efficient and high-performance active suspension systems in future vehicles.

## ACKNOWLEDGMENTS

This work was supported in part by the U.S. Department of Energy, Office of Science, Office of Workforce Development for Teachers and Scientists (WDTS) under the Science Undergraduate Laboratory Internships program.

## REFERENCES

- [1] Mamadou Mboup, Cédric Join, and Michel Fliess. “Numerical Differentiation with Annihilators in Noisy Environment”. In: *Numerical Algorithms* 50 (Apr. 2009). DOI: 10.1007/s11075-008-9236-1.
- [2] Zejiang Wang and Junmin Wang. “Ultra-Local Model Predictive Control: A Model-Free Approach and Its Application on Automated Vehicle Trajectory Tracking”. In: *Control Engineering Practice* 101 (Aug. 2020), p. 104482. ISSN: 0967-0661. DOI: 10.1016/j.conengprac.2020.104482. (Visited on 06/24/2024).
- [3] Zejiang Wang, Xingyu Zhou, and Junmin Wang. “Extremum-Seeking-Based Adaptive Model-Free Control and Its Application to Automated Vehicle Path Tracking”. In: *IEEE/ASME Transactions on Mechatronics* 27.5 (Oct. 2022), pp. 3874–3884. ISSN: 1941-014X. DOI: 10.1109/TMECH.2022.3146727. (Visited on 06/25/2024).